

RESEARCH

Open Access



# A novel workflow for geothermal exploration: 3D seismic interpretation of biohermal buildups (Upper Jurassic, Molasse Basin, Germany)

Philipp Wolpert<sup>1\*</sup> , Thomas Aigner<sup>2</sup>, Daniel Bendias<sup>3</sup>, Kilian Beichel<sup>3</sup> and Kai Zosseder<sup>4</sup>

\*Correspondence:  
pwolpert@v-er.eu

<sup>1</sup> Vulcan Energy Subsurface Solutions GmbH, An Der Raumfabrik 33C, 76277 Karlsruhe, Germany

<sup>2</sup> Eberhard Karls University Tübingen, Sedimentary Research Group, Hölderlinstr. 12, 72074 Tübingen, Germany

<sup>3</sup> SMW Stadtwerke München, Emmy-Noether-Straße 2, 80992 Munich, Germany

<sup>4</sup> Chair of Hydrogeology, Technical University of Munich, Arcisstr. 21, 80333 Munich, Germany

## Abstract

The Upper Jurassic carbonates are the prime target for deep geothermal exploration in the Molasse basin, South Germany. The carbonates have a thickness of over 500m (1640 ft) and consist of two major facies: (1) bedded marly limestone and (2) massive limestone and dolostone. The massive limestone facies is composed of sponge-microbial biohermal buildups. It is considered the main geothermal reservoir facies. Only this facies type may be (1) karstified, (2) dolomitized, and/or (3) faulted and fractured, and therefore can yield very high flow rates of >100 l/sec = 26 gpm. The main data source used in this study is the 3D seismic survey of the Freiamt geothermal field in the western part of Munich/Germany. Blended in were cutting logs to describe the lithology from 2 wells and borehole image logs from the two geothermal wells. Lithologies derived from these wells were upscaled in support of the seismic interpretation. The study presents an integrated workflow of 3D seismic attribute analysis to analyze the distribution and quantification of reservoir facies (massive limestone) versus non-reservoir facies (bedded marly limestone) per time slice. The attribute “sum of magnitude” is mapped for 9-time slices based on the vertical resolution of the Freiamt 3D cube. The seismic facies interpretation is compared with upscaled borehole image facies associations of two geothermal wells. BHI log data is calibrated with an interpretation of the depositional environment based on cutting analysis. Reservoir geometries were derived from an outcrop analog study to better understand the 3D seismic facies interpretation and to construct the conceptual depositional model of the Upper Jurassic carbonates. This technique is commonly used in hydrocarbon exploration but is not yet adapted to geothermal projects, which are often based on little data, smaller company sizes, tight budgets, and limited access to specialized geomodelling software and experience. The approach of using 3D seismic attribute analysis presented in this study provides a quantitative subsurface model of geothermal reservoir facies in the Freiamt geothermal field. It is quick and straightforward and can easily be applied in the exploration workflow for similar fields and reservoirs.

**Keywords:** Geothermal exploration, Carbonates, Seismic attribute analysis, Sequence stratigraphy, Upper Jurassic, Molasse basin, Germany

## Introduction

Geothermal projects are implemented in the city of Munich to provide citizens with green domestic heating by 2040 and to cover Munich's electricity demand by 2025 (<https://www.swm.de>). Munich is located in the Southern German Molasse basin, which is known for elevated geothermal gradients. The aquifer are Upper Jurassic carbonates are the focus of geothermal exploration. Table 1 shows the stratigraphic Jurassic sequence of south Germany. Upper Jurassic carbonates are buried to a depth of 2500–4000m (9800–1300ft) in the Munich metropolitan area. The regional structural dip is towards the South Alpin deformation front. The focus area of this study is the area covered by the 3D seismic survey 'Freiham', located in the western part of the city of Munich (Fig. 1). Two geothermal wells 'Freiham TH1' (producer) and 'TH2 (injector)' have been drilled in the area. The wells feed into a geothermal power plant. It provided sufficient energy to supply the district of Freiham and surrounding areas with domestic heating since 2016 (<https://www.swm.de>). Because geothermal projects tend to run on a tight budget only sparse datasets are acquired. For example, an exploration well was not drilled. The aim of this study is to extract geological information from this producing geothermal field and use these insights to de-risk follow-up prospects in the area. The Freiham field provides the opportunity to calibrate seismic attributes with well logs and cuttings to build a rock-calibrated subsurface model as shown in Table 2. The aim of this study is to extract geological information from this producing geothermal field and use these insights to de-risk follow-up prospects in the area. The Freiham field provides the opportunity to calibrate seismic attributes with well logs and cuttings to build a rock-calibrated subsurface model. The objective is to differentiate biohermal buildups, the commonly karstified and dolomitised potential reservoir from marly inter-buildup non-reservoir facies using calibrated seismic attributes. The method has its limitations. It is not suited to characterize faults or fracture zones. Prominent fault zones were the primary target of adjacent geothermal projects such as in the town of Geretsried or the town of Mauerstetten. The geological concept suggested high permeability which was associated with structural features only. However, the wells targeting fault permeability were not successful and the project failed (Dussel et al., 2018) due to orientation to the stress regime, diagenesis, clay smear in marly facies.

## Geological setting

During the Upper Jurassic, large parts of the continental edges were flooded, forming epicontinental shelf seas (Ziegler 1990; Scotese 2001; Blakey 2015) (light blue rims of

**Table 1** Stratigraphic overview of the Upper Jurassic carbonates in Southern Germany

Series	Stage (ICS) international	Lithostratigraphy	Age (Ma) chronostratigraphic	Reservoir zones
Upper Jurassic (Malm)	Tithonian	Zeta 1–6	150.8–145.5	Potential reservoir
	Kimmeridgian	Epsilon	155.6–150.8	
		Delta 1–4		Non-reservoir
		Gamma		
	Oxfordian	Beta	161.2–155.6	
		Alpha		

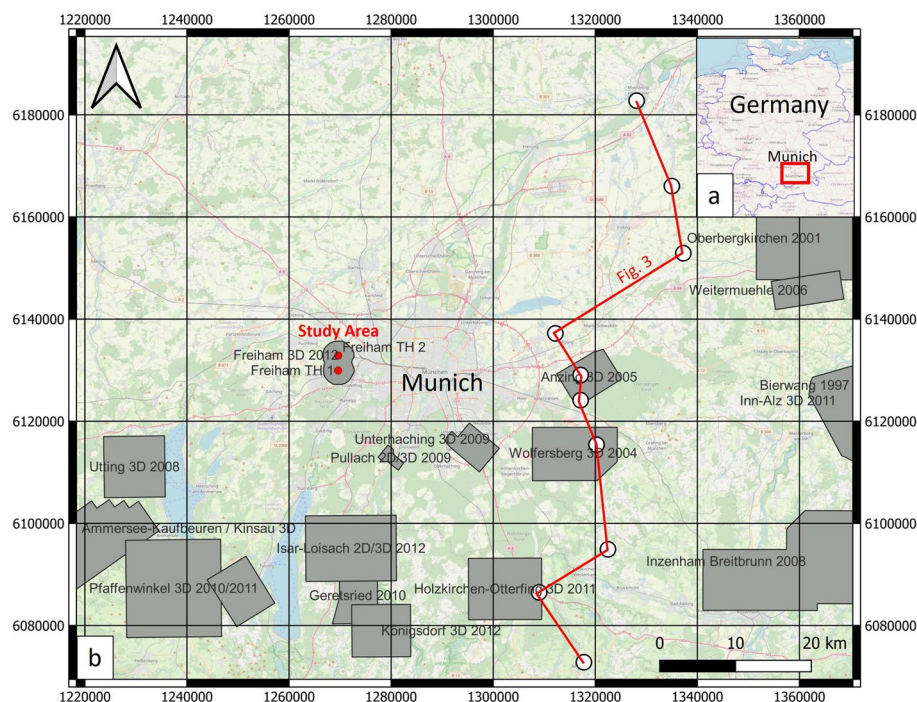


**Fig. 1** **a** Map of Germany with the greater Munich area marked by the red square. This area is under intensive geothermal development. **b** The map shows the study area and the location of the Freiham geothermal project with the two geothermal wells (Freiham TH1 = producer and TH2 = injector) and the area of the 3D seismic survey (grey). Additionally, other 3D seismic surveys are highlighted with potential for geothermal exploration and further development. Figure 3 shows a North–South cross-section

**Table 2** Available database used in this project

Type of data	Length/size	Properties
3D seismic survey	4.2 km × 5.5 km	Final pre-stack depth migrated (time)
Well Freiham Th1	E.T. 3130 m (MD)	CMI-Logs, GR, CAL, Mudlog, Temp, ROP
Well Freiham Th2	E.T. 2600 m (MD)	CMI-Logs, GR, CAL, Mudlog, Temp, ROP
Cuttings from Th2 and Th1	265 samples	Cutting-based facies analysis

continents; Fig. 2). The Upper Jurassic of South Germany was part of such an epicontinental shelf. To the North, the shelf was separated from the boreal sea by an island archipelago and connected to the Tethys Ocean in the South (Meyer and Schmidt-Kaler 1989, 1990; Meyer 1994). The Upper Jurassic sequence shows an overall shallowing-up trend and consists of two major lithofacies associations that are (1) well-bedded limestones and (2) massive limestones (Gwinner 1976; Geyer and Gwinner 1979; Ziegler 1977). The massive limestones are mainly composed of sponges, thrombolites, and microbial crusts, formed in a relatively deep shelf environment (below storm wave base) as bioherms or mounds (Geyer and Gwinner 1979; Ziegler 1977; Meyer and Schmidt-Kaler 1989; Leinfelder 1993; Leinfelder et al. 1994, 1996; Pawellek and Aigner 2003a). During the further evolution, the sponges as a main-bioherm builder are commonly replaced by corals. Furthermore, the presence of ooids, peloids, and reef debris in the uppermost



**Fig. 2** Detail view of the Late Jurassic showing the northern edge of the Tethys ocean, the opening of the Central Atlantic Ocean, and the surrounding landmasses (Blakey 2015). During the Upper Jurassic, up to 600-m-thick carbonates were deposited in South Germany, with a simplified North-East/South-West proximal–distal trend

part can be observed, indicating a shallower environment of deposition (Strasser and Davaud 1983; Strasser 1986; Meyer and Schmidt-Kaler 1989, 1990; Meyer 1994). Clastic input (clay) was derived from the Rhenish Massif in the North (Gygi 1986; Meyer and Schmidt-Kaler 1989) and partly from the Swiss Platform in the West (Pittet and Strasser 1998; Pittet et al., 2000). Figure 2 provides a large-scale overview of the Upper Jurassic proximal–distal trend, which has important implications for the geothermal developments too. Permeable karstified carbonate buildups (greater Munich area) grade into a more distal depositional environment towards the southwest, characterized by unsuccessful geothermal wells like Geretsried and Mauerstetten (Dussel et al. 2018).

The Molasse basin formed during the late stages of the Alpine orogeny. It represents a typical asymmetric foreland basin that dips to the south and continues at least 50 km underneath the nappes of the Alps (Bachmann et al. 1987). Figure 3 shows a North–South oriented cross-section (Lemke 1988). Hence, the Upper Jurassic Malm carbonates are buried deep enough to reach high geothermal gradients in the greater Munich area, and even higher temperatures further to the South. The basement is of Variscan age and consists of gneisses and granites (Bachmann et al., 1991). They were uplifted and eroded during the Late Carboniferous resulting in an SW–NE oriented graben and troughs system (Ziegler, 1990; Ziegler and Dèzes, 2006). During the Jurassic, these preexisting basement structures were reactivated (extensional phase), resulting in differential subsidence and rotation of fault-bounded blocks (Wetzel et al., 2003).

The Upper Jurassic Malm of South Germany has been subject to numerous studies predominantly in outcrops of the Swabian and Franconian Alb (e.g., Quenstedt 1858; Gwinner 1976; Ziegler 1977; Geyer and Gwinner 1979; Leinfelder 1993; Leinfelder et al. 1994, 1996; Meyer and Schmidt-Kaler 1989, 1999; Pawellek and Aigner 2003a, 2003b; Ruf et al. 2005). In the period of 1980–1990, the Molasses basin was



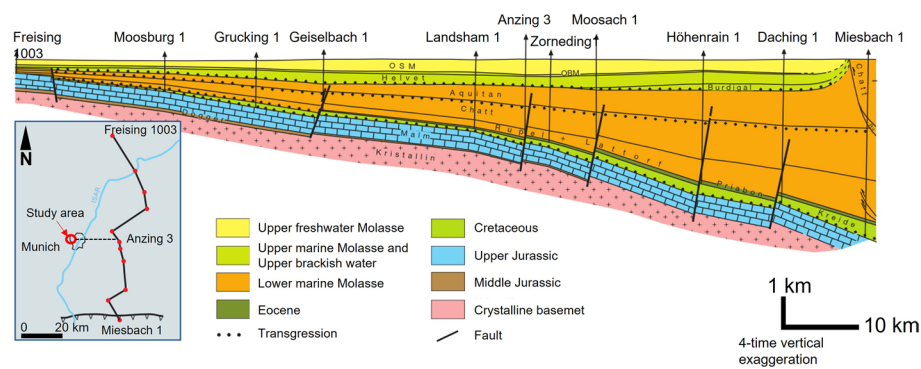


**Fig. 3** N–S cross-section of the Molasse basin (Lemke 1988). It shows the asymmetric geometry of a typical foreland basin that is dipping to the South towards the Alps. The geothermal reservoirs of the Upper Jurassic carbonates (blue) are therefore buried deep enough in the greater Munich area to reach attractive temperatures for heat and further south even for combined heat and power production

actively explored for hydrocarbons and abundant subsurface data like seismic profiles (2D), wireline logs, and cores were acquired. The paleogeographic maps from Meyer and Schmidt-Kaler (1990) are based on fieldwork and subsurface data and provide basic information on the development and distribution of the Upper Jurassic in South Germany. A sequence stratigraphic framework for the complete Upper Jurassic is not yet established. A reason for that being is that large parts are deposited in a relatively deep carbonate ramp/platform, in general, situated below the average storm wave base (Pawellek and Aigner 2003a). Classical sequence stratigraphic surfaces, such as sequence boundaries (Van Wagoner et al. 1988, 1990; Hanford and Loucks 1993) tend to be only poorly developed. Even so, sequence stratigraphic interpretation in this deep-water realm of the Upper Jurassic is still possible as shown by Pawellek and Aigner 2003a, 2003b, 2004; Ruf et al. 2005; Pross et al. 2006. The key to unlocking the sequence stratigraphic development is not to search for sharp stratal surfaces, but to focus instead on transitional facies shifts referred to as “turnarounds” (Schlager 1993; Kerns and Tinker 1997). Figure 4 shows the research well Moosburg SC4, located approximately 45 km north-east of Munich, close to the town Moosburg an der Isar. It is the only fully cored well through the entire Upper Jurassic of South Germany (TD 1585, 20 m). The cored interval contains: (1) 18 m of the Middle Jurassic Dogger (including the glauconitic marker bed), (2) 453 m of the Upper Jurassic, and (3) 134 m of the Upper Jurassic/Lower Cretaceous Purbeck Formation. The well has been initially studied and interpreted by Meyer (1994). Böhm et al. (2011) and Böhm et al. (2013) analyzed the different types of dolomite of the Upper Jurassic interval based on thin section. Classification after Dunham (1962) and detailed sedimentological logging on a 1:20 scale further revealed 22 facies types for the Upper Jurassic and Purbeck Formation (Wolpert et al. 2019a). Following the methodology and nomenclature after Catuneanu et al. 2011, four large-scale depositional sequences (S1–4) were interpreted, as shown in Fig. 4. Based on local knowledge and several 2D correlation lines, the large-scale sequence stratigraphic architecture of research well Moosburg SC4 can be transferred into the subsurface of the greater Munich area (Wolpert et al., 2019a.) although S4 is only partly preserved or absent due to

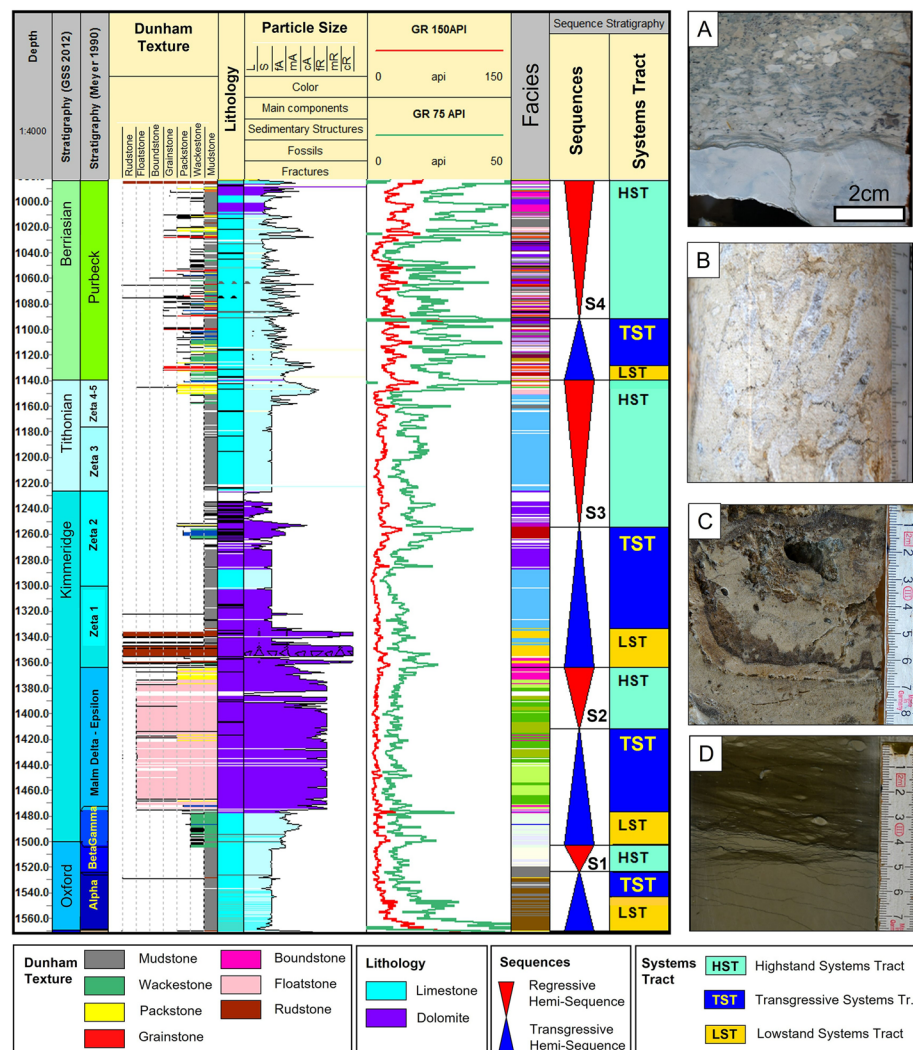


**Fig. 4** Sequence stratigraphic interpretation of the Upper Jurassic based on the fully cored research well Moosburg SC4. Sequence 1 (S1) is mainly dominated by dark, clay-rich mudstones **D**. Sequence 2 (S2) is largely comprised of dolomitic sponge-thrombolite floatstone, which is considered an important reservoir facies **C**. During the HST of sequence 3 (S3) a shift to shallow water and partly high-energy facies is observed as the sponges are gradually replaced by corals **B**. Bioherm/reef debris wedges, extending several 100's m into the basin, are frequently observed on the 3D seismic and interpreted as highstand shedding (Schlager et al. 1993). Sequence 4 (S4) shows multiple exposure surfaces (**A**) and dolomitic intervals and marks a gradual change into a terrestrial system with the presence of silt and sandstone

erosion during the Cretaceous. The value of information derived from the fully cored research well is significant because none of the geothermal projects in the Munich area could take continuous core samples from the reservoir section (budget and technical circumstances).





The highest flow rates are encountered in the Upper Jurassic carbonates in the area of interest if these are: (1) karstification, (2) dolomitization, and (3) faults/fractures. The distribution of stratigraphic-related reservoir zones is described below in Fig. 5.

Productive fractures form predominantly in harder lithology and facies (Mattioni et al. 2009). Borehole image logs from wells Freiham Th1 and Th2 revealed a stronger

fracture intensity in brittle facies such as massive limestones and dolostones. In contrast, fractures cannot propagate as far and are often affected by clay smears in ductile marls and the well-bedded marl-limestone alternations (Wolpert and Pöppelreiter 2019). Faults and related fracture zones are the main targets for geothermal exploration in the Molasse Basin when interpreted in the context of stress orientation, fault offset, size of the fault damage zone, juxtaposition, potential clay-smear, and other characteristics into account. However, a pre-defined wellsite/power plant location (due to the existing infrastructure) may prevent access to suitable structural features. For example, only one larger fault zone can be accessed in the Freiham area. Thus, alternative reservoir types are considered that might be multiple stratigraphic targets and karstified horizons.

### Dataset

The Molasse Basin has been actively explored for hydrocarbons in 1980-90. Abundant subsurface data such as seismic profiles (2D), wireline logs, and cores were acquired. Figure 5 summarizes the available data for this study. It provides a unique dataset for a geothermal project in the Molasse Basin, including 3D seismic, two geothermal wells with check-shots, borehole images, mud and wireline logs, and cuttings. The latter was used to prepare thin sections, and to analyze microfossil assemblages. The

Purbeck (Uppermost Jurassic/ Cretaceous)	Sequence 4	HST		Dominated by shallowing upward cycle motives and multiple exposure surfaces, often associated with karstification. Due to erosion and uplift in the Cretaceous, the Purbeck Formation is only partly and localized preserved in the subsurface of the greater Munich area.
		TST		Non-reservoir
		LST		Non-reservoir
	Sequence 3	HST		Gradual change to shallower water, high energy facies. Due to reduced accommodation space and a high carbonate production, the bioherms/reefs shed debris into the basins, which can be prolific flow zones. The SB Top Jurassic represents a major karst event/interval and is a significant flow zone.
		TST		Non-reservoir
		LST		Non-reservoir
	Sequence 2	HST		The late HST-SB is usually intensively karstified and represents a significant flow zone.
		TST		The TST (Malm delta interval) contains a very prolific reservoir facies, the dolomitic sponge-thrombolite floatstone. Dolomitization created inter-crystalline porosity and abundant vuggy porosity. Permeability is usually high.
		LST		
	Sequence 1	HST		Non-reservoir due to the high amount of clay (aquitards)
		TST		
		LST		

**Fig. 5** Simplified main geothermal reservoir facies distribution in a sequence stratigraphic context. It shows that stratigraphic-related flow zones are in general following sea level-related trends that can be characterized by the sequence stratigraphic framework

holistic interpretation and integration of these various datasets allow a correlation of discrete stratigraphic units and sub-units with seismic reflectors.

The seismic data set used for interpretation was processed using a Kirchhoff pre-stack depth migration workflow with no post-processing filters being applied. The raw full stack cube was identified as most suitable to ensure that true amplitudes are preserved and not impacted by post-processing and was hence used. The seismic cube covers an area of about 23km<sup>2</sup> and contains 417 inlines, 425 crosslines with a bin size of 25 m, and a sampling rate of 4 ms.

Figure 6 shows the frequency spectrum of the interval of interest (1200–1600 ms) used to estimate the vertical and lateral resolution. The dominant frequency spectrum is 10–60 Hz. The velocity for the carbonate rocks is 5000–5500 m/s derived from regional velocity data provided by Erdwerk. The theoretical resolution limit is calculated using the following equation  $\lambda = v/f$  ( $\lambda$  = lambda/wavelength;  $v$  = velocity;  $f$  = frequency). As a result, we get  $\lambda = 83$  m–92 m and  $1/4 \lambda = 20$  m–23 m as a theoretical resolution limit. However, considering noise and other effects, we estimate a vertical and lateral resolution of 25–30 m as more realistic.

From the SEG-Y-header the following information was retrieved: The bin spacing is 25 m in in-line and crossline directions. The polarity of the seismic dataset is SEG positive, so positive amplitudes correspond to relative changes from a layer of lower to higher acoustic impedance. The phase of the reflection data set is zero phase. The color palette used in displaying the dataset corresponds to: blue = soft kick, yellow = hard kick and white = 0-intersection). The well ties of Freiham 1 and 2 were conducted by Erdwerk using checkshot data from each well. Offset wells were incorporated to establish regional velocity trends and used for QC. Microfossil assemblages in cuttings were used to identify the different stratigraphic units. No core or sidewall cores were taken.

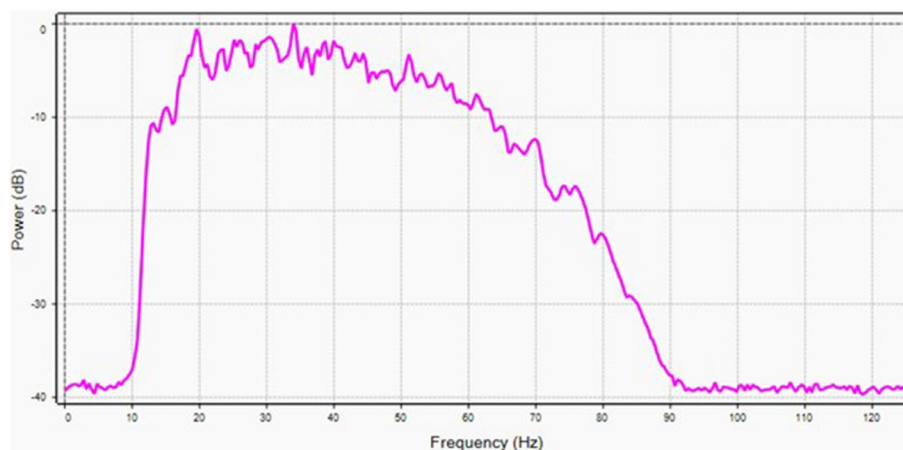


**Fig. 6** The frequency spectrum of the interval of interest shows that the dominant frequency spectrum is between 10 and 60 Hz



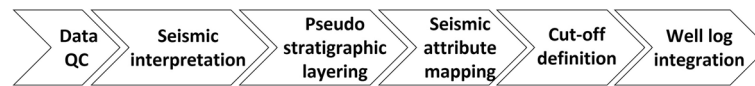


**Fig. 7** Schematic visualization of the applied workflow used in this study

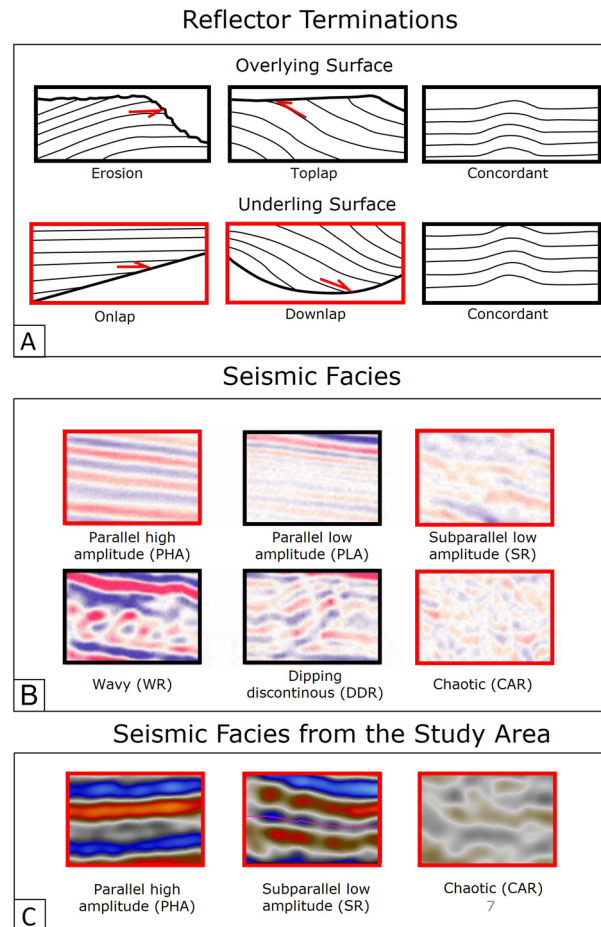


**Fig. 8** **A** Reflector termination classification and **B** seismic facies and after Mitchum et al. (1977). Marked in red are the most frequently occurring features in this study: parallel high amplitude (PHA), subparallel low amplitude (SR), and chaotic (CAR), as well as onlap and downlap seismic surfaces. **C** Examples of seismic facies observed in this study

## Workflow

The workflow applied in this study is summarized in Fig. 7 Each step is explained in detail in the following sections.

## Seismic interpretation

The first step of the seismic interpretation is the seismic-well tie procedure. In our study, this work has been performed by geoscientists from the company Erdwerk. Check-shots from both wells were used. The results were compared with offset wells and regional seismographic correlations from other geothermal projects in the Munich area, as well as hydrocarbon wells which have typically a more comprehensive logging suit including

sonic and density logs (which are not common in most geothermal wells). The second step of the workflow follows the standard seismo-stratigraphic interpretation (Mitchum and Vail 1977; Vail et al. 1977; Vail, 1987) and consist of: (a) seismic facies analysis and (b) reflector terminations mapping as shown in Fig. 8. Three seismic facies types are pronounced and frequently observed in this study: (1) parallel high amplitude (PHA), (2) chaotic (CAR), and (3) subparallel low amplitude (SR). Common reflector terminations are onlaps and downlaps.

Figure 9 shows an example of an uninterpreted and interpreted seismic line. Acquisition of wireline logs is kept to a minimum for economic reason in most geothermal projects. Thus, there are no sonic or density logs available. The seismic to well tie is typically performed via check-shots. The parallel high amplitude seismic facies is interpreted as well-bedded limestones which is deposited in the basin. The chaotic seismic facies is interpreted as bioherm/reef. The basin facies shows onlaps onto bioherm/reef. The subparallel low amplitude (SR) seismic facies, together with wedge shape geometries, are interpreted as possible debris apron surrounding bioherm/reef. The vertical stacking of the facies was analysed in a seismic sequence stratigraphic context. Three large-scale sequences (S1–S3) were differentiated (S1–S3) (Wolpert et al. 2019b). A similar stacking

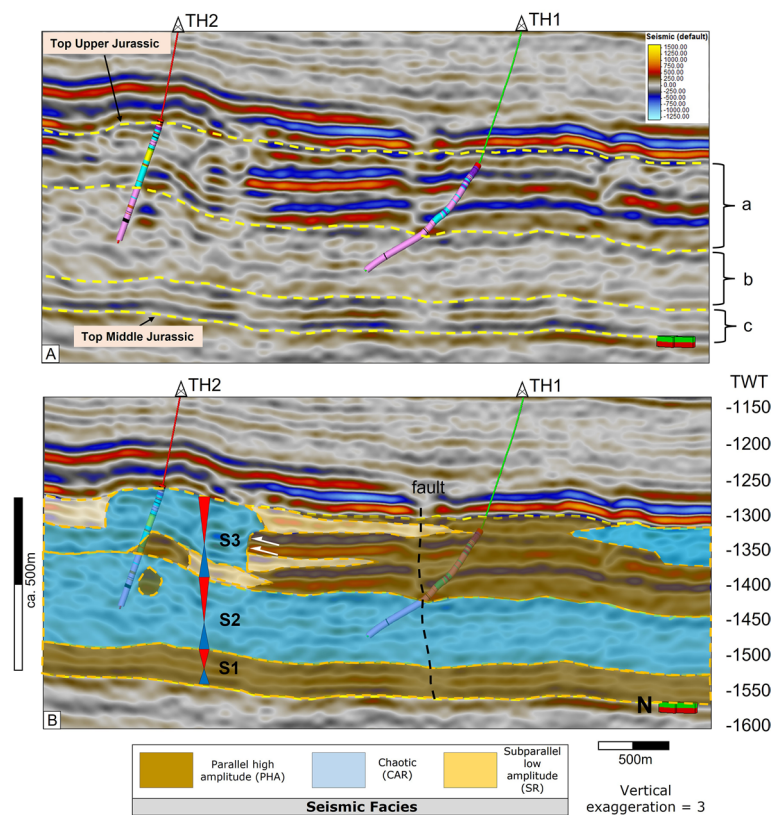


**Fig. 9** Seismic line showing the uninterpreted (A) and interpreted (B) section. The wells Th2 and TH1 confirm the Top Upper Jurassic and the Upper Malm unit (a), as well as part of the Middle Malm unit (b). Lower Malm unit (c) and Top Middle Jurassic cannot be confirmed by the two wells. The interpretation is, however, supported by offset wells and other geothermal projects in the Munich area. Seismic facies analysis and reflector terminations show basin, reef/bioherm, and reef/bioherm debris as well as three large-scale depositional sequences (S1–S3) and a fault

pattern was identified in borehole image facies interpretation and confirms S3 and the regressive hemi-sequence of S2. Seismic facies, reflector termination mapping, and sequence stratigraphic interpretation reflect the large-scale depositional architecture of the Upper Jurassic (Gwinner 1976; Geyer and Gwinner 1979; Meyer and Schmidt-Kaler 1990; Meyer 1994; Böhm et al 2011);

### Pseudo-stratigraphic layering

A quick and elegant way to subdivide the area of interest in a 3D seismic cube is a pseudo-stratigraphic layering approach (depth slices) (Bendias and Contreras 2017). To extract seismic properties from stratigraphically meaningful slices, the zones need a thickness that is consistent with the seismic vertical resolution of about 25 ms. Thus, each slice should contain one positive and one negative amplitude. Figure 10 A shows Top Upper Jurassic and Top Middle Jurassic. These stratigraphic tops are two interpreted seismic surfaces. The surfaces between Top Upper Jurassic and Top Middle Jurassic are isochored based on the total thickness and constrained by seismic events (Fig. 10 B). The zone between the pseudo-stratigraphic layers should resolve one peak and trough (positive and negative amplitude) of the seismic wave.

### Seismic attribute mapping per zone

Seismic attributes are measurements calculated from the seismic volume, which are sensitive to wave kinematics/dynamics or reservoir features. Attributes calculated include amplitude, waveshape, frequency, energy, and attenuation. Different seismic attributes like root mean square (RMS) amplitude, envelope (reflection strength), instantaneous frequency, and many more may highlight certain reservoir properties (fault geometries, karst and subsurface anomalies (e.g., Braun 1996; Chen and Sidney 1997; Chopral and Marfurt 2005); Results from the seismic facies analysis in this study showed that the strength of the reflectors correlate very well with the seismic facies. The chaotic seismic facies has a weak reflectivity while the parallel high-amplitude facies shows a strong reflectivity. Therefore a seismic attribute that describes the strength of the amplitudes is required. The “sum of magnitude” attribute

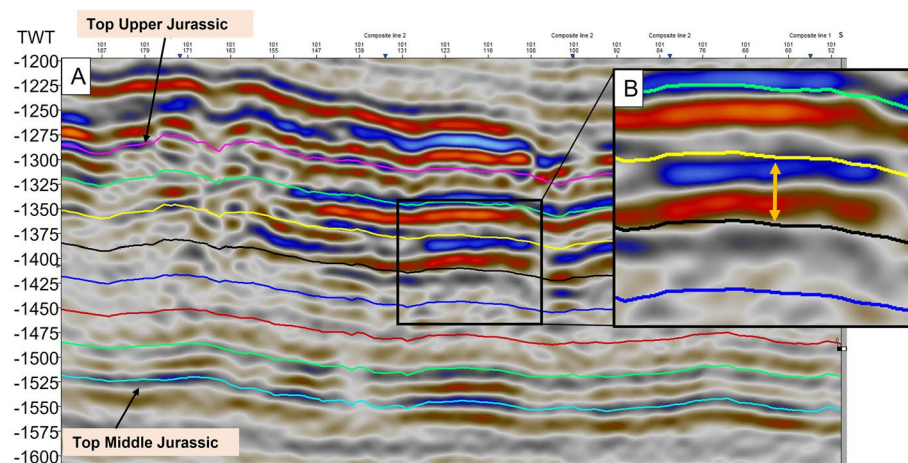


**Fig. 10** A Top Upper Jurassic and Top Middle Jurassic are interpreted surfaces, whereas the layers in between are calculated based on the thickness map and seismic resolution as shown in B. In this way, each slice should contain one positive and one negative amplitude. This pseudo-stratigraphic layering scheme allows to quickly create surfaces that can be used in the further steps of the workflow

is an indicator for reflectivity, no matter if the values are positive or negative (peak or trough). If the “sum of magnitude” attribute yields high values, a high reflectivity is present. The high reflectivity corresponds to the parallel high amplitude seismic facies, interpreted as basin. Vice versa, the low values correspond to a low reflectivity and represent the chaotic seismic facies, interpreted as reef/bioherm which equals the potential geothermal reservoir facies.

Seismic attributes were mapped per zone, as defined by the pseudo-stratigraphic layering. Figure 11 shows the result of the “sum of magnitude” attribute for zone 1. The purple colors are areas of high reflectivity, red and yellow represents low reflectivity. The first impression of the attribute maps is very promising, as general trends and geometries can be recognized. However, the link between the values of the attribute map and the actual seismic facies still has to be established.

### Cut-off definition

Defining the threshold is a critical step to convert the attribute maps into a meaningful geological tool. Hence, the cut-off definition is fundamental to differentiate between the parallel high amplitude seismic facies and the chaotic seismic facies (basin vs. bioherm/reef). The best practice is working with a split-screen mode and enabling “cursor tracking mode” in the interpretation software (Fig. 12, A and B, orange cursor). The attribute map is now compared with the seismic line. Critical features like onlaps of the parallel high amplitude facies (basin) with the chaotic seismic facies (bioherm/reef) are used to define the cut-off. Figure 12 C shows the histogram of the “sum of magnitude map” for zone 1, with the defined cut-off between bioherm/reef and basin. For this zone, every “sum of magnitude” value > 900 corresponds to the high amplitude seismic facies (basin), and every value less than 900 corresponds to the chaotic seismic facies (reef/bioherm).

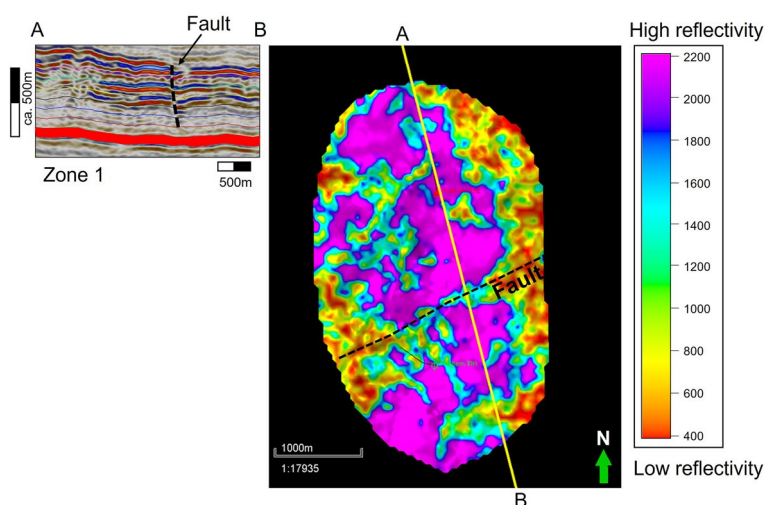


**Fig. 11** Seismic attribute mapping per zone. The example shows the first results for zone 1, with high reflectivity in purple and low reflectivity in yellow/red colors. The high reflectivity correlates with the parallel high-amplitude seismic facies, which is interpreted as the well-bedded basin facies, and the low reflectivity correlated with the chaotic and subparallel low amplitude seismic facies. However, the cut-off between the two end-members needs to be defined in the next steps



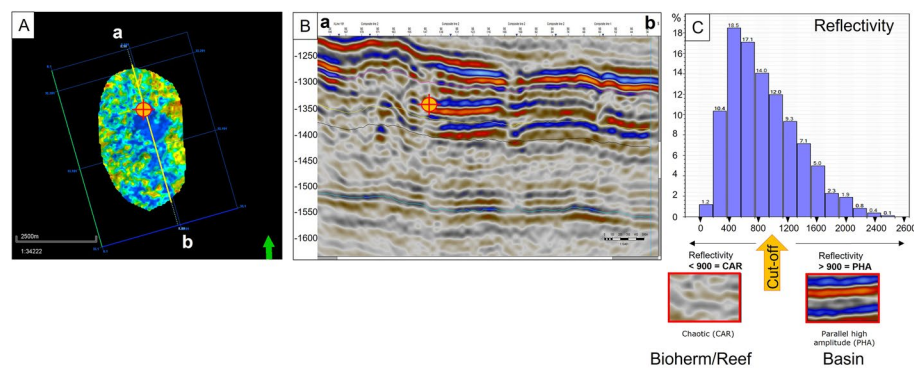


**Fig. 12** Cut-off definition via cursor-tracking mode and visual comparison. **A** adjusted attribute map compared simultaneously with the seismic line (**B**) to define the threshold for basin and reef/bioherm and basin (**C**). This visual and iterative approach is used to define the cut-off value and works best at the onlaps of the parallel high-amplitude seismic facies with the chaotic facies. It needs to be adjusted for each time slice using multiple inlines and crosslines. The upscaled image facies interpretation from the 2 geothermal wells supports the correlation of the seismic facies with the deposition environment (basin facies or bioherm/reef facies)

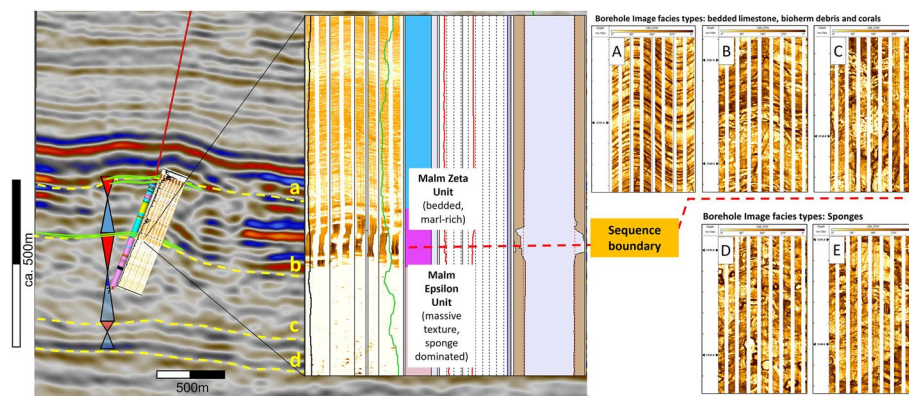


**Fig. 13** The upscaled BHI facies is used to validate certain aspects of the seismic facies interpretation and to confirm the depositional environment. The lower part of the static borehole image log is much more resistive and homogeneous than the upper part. The dynamic image reveals that sponges dominate this interval and are the main recognizable bioherm-building organisms (**E, F**). This supports the seismic facies interpretation and confirms furthermore the sequence boundary, which is a karstified flow-zone. The upper part of the borehole image log is heterogeneous and more conductive. Intervals of well-bedded limestone (**A**), bioherm debris (**B**), and corals towards to top of the section (**C**) can be observed. This supports the general shallowing upward trend towards the end of the Upper Jurassic and also supports the seismic facies interpretation

This process needs to be repeated for various inlines and crosslines, and then for every zone to adjust the cut-offs accordingly.

### Integration with BHI logs, cuttings and outcrop

Borehole images (in the study area CMI tools) were acquired in the geothermal wells, as well as borehole cuttings and thin sections thereof. Although borehole image interpretation in carbonate reservoirs is very challenging, which is caused by low internal resistivity contrast (e.g., Akbar et al. 1995; Chitale et al. 2010; Steiner and Böhm 2011) a large amount of detail was found to be visible in the available dataset. It even allows distinguishing between various bio-components such as corals and sponges,

reef debris, and many distinctive features. Cuttings and thin sections were further used to validate the borehole image facies interpretation (Fig. 13). The borehole image facies interpretation could be used with confidence to verify the depositional environment and was upscaled accordingly into the main facies associations to match the vertical seismic resolution of 25 to 50 ms which translates into 50 to 60 m (Wolpert et al, 2019b). It confirms that the chaotic seismic facies (CAR) correlated with the bioherm/reef facies association, and the parallel high-amplitude seismic facies (PHA) with the well-bedded basin facies. The presence of bioherm/reef debris could only be partly be verified, as the well path does only perforate the outer edge of the interpreted debris wedge. However, for the purpose of this study and the resolution of the attribute maps, the main objective was to differentiate between the two end-members “bioherm/reef” and “basin” which could be confirmed by the integration of the borehole image logs.

Outcrops analogs of the Swabian and Franconian Alb provide the opportunity to compare the seismic interpretation with dimensions and geometries derived from field observations. Figure 14 shows an example that further supports the seismic interpretation of some key features such as onlaps of the basin facies onto the bioherm/reef, reef debris wedges (100 s of meters scale), and the well-bedded basin facies (Pawellek and Aigner 2003a; Ruf et al. 2005). More detailed studies on bioherm buildups and lateral heterogeneities from the Swabian Alb via satellite images combined with field work support the seismic interpretation of this study (Chiracal 2020).

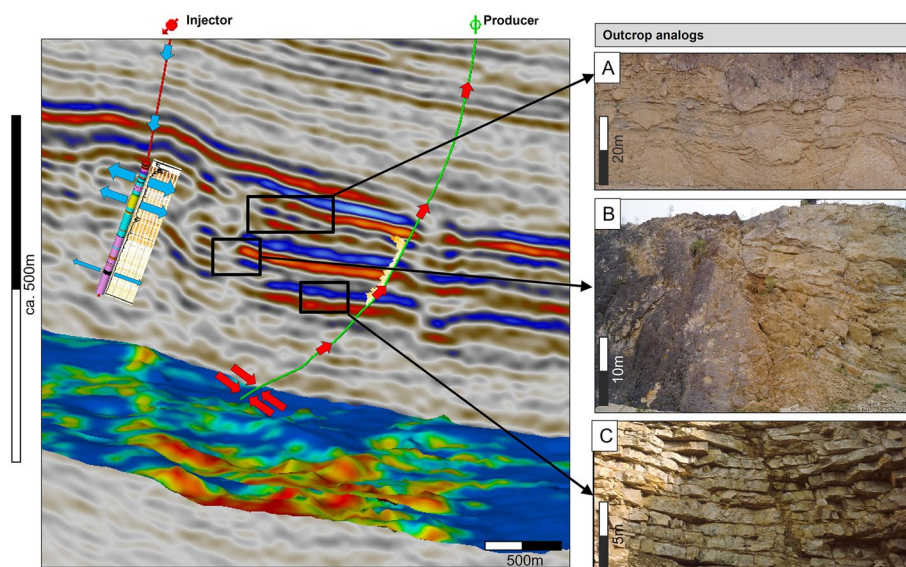


**Fig. 14** Conceptual comparison of the three dominating seismic facies types interpreted in this study with outcrop analog observations of the Upper Jurassic outcrops from the Swabian Alb. **A** bioherm/reef debris (= subparallel low amplitude seismic facies) comprised of large olistoliths can be up to 40–50 m thick and are typically present during the (late) HST of sequence 3. **B** Onlaps of the well-bedded basin facies (= parallel high-amplitude seismic facies) onto the bioherm/reef buildups (chaotic seismic facies) show a very sharp contact and can be frequently observed in the field. **C** Well-bedded limestone with frequent clay–marly alternations interpreted as basin facies observed in the outcrop and interpreted as parallel high-amplitude seismic facies

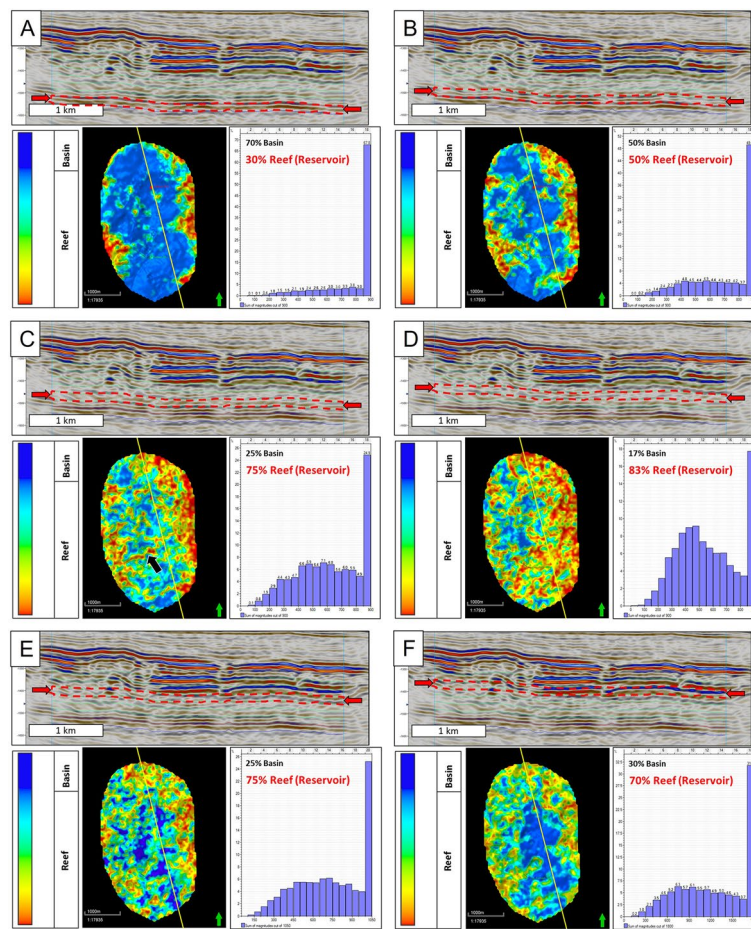


**Fig. 15** Sum of magnitude maps from base to top (A–F). The yellow line shows the orientation of the seismic section. The adjusted maps reveal now the percentage of basin facies and bioherm/reef facies (potential geothermal reservoir facies). It shows how the amount of reservoir facies is increasing from map A to D which represents the large-scale progradation of sponge-dominated bioherms during this period. Map D is also a turning point, as the amount of reservoir facies is declining now

### Results of the attribute mapping: quantification of reservoir facies vs. non-reservoir facies

The following Figs. 15, 16 show the results of the adjusted “sum of magnitude” attribute maps from bottom to top and per zone. The histogram allows quantifying the parallel high-amplitude seismic facies (basin) and the chaotic seismic facies (bioherm/reef) and hence provides a proxy of potential reservoir vs. non-reservoir distribution per zone. Zone A contains only 30% of bioherm/reef and shows furthermore that it might be very challenging to reach those potential targets from the available predefined well sites, although these targets might have the hottest reservoir temperatures. (B) The amount of bioherm/reef is constantly increasing and progradation can be observed, especially from the NE. The intra-basins are gradually disappearing. (C) Only small remains of the intra-basins are visible and the sponge-dominated bioherms are further striving and prograding, predominantly from the NE and E. The black arrow indicates a NE–SW-oriented feature, which is not a bioherm/reef. It is caused by the NE–SW striking fault, which has a chaotic seismic facies envelope, and is therefore classified as bioherm/reef using the “sum of magnitude” method. This is a limitation of the presented method.



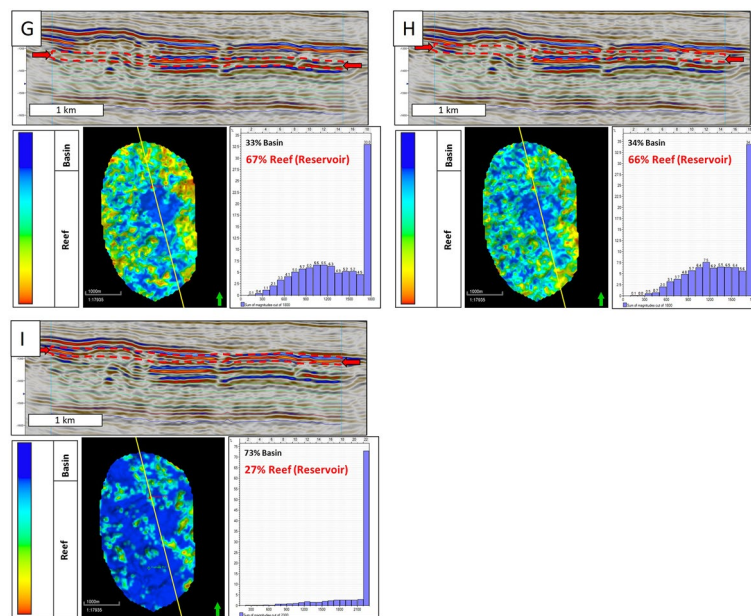


**Fig. 16** Sum of magnitude maps from base to top (G–I) show how the amount of reservoir facies is declining dramatically. It shows furthermore the geometries of the biohermal buildups (reservoir facies) and the orientation of smaller intra-basins. Especially the upper section of the buildups is prone to karstification and a shift to shallow-water facies which could be confirmed by the borehole image logs

(D) The bioherm/reefs reach a maximum of 83% in zone 4, which corresponds to the maximal expansion of bioherm/reef growth as known from outcrop studies (Leinfelder 1993). This interval can represent a very prolific geothermal reservoir zone and the maps show also first impressions of the geometries and orientation. The maps show also that the main sediment input was derived approximately from the N–E/E which is important to know when targeting biohermal debris wedges, or when thinking about facies distribution and facies modeling. Maps E, F, G, and H show the formation of the intra-basins and the pronounced geometries of the buildups. Especially the buildups represent prime geothermal targets, as the tops can be frequently karstified and dolomitized. During highstand shedding, bioherm/reef debris was deposited into the surrounding intra-basins and can represent potential geothermal targets as well. From then onwards the amount of bioherm/reef gradually decreases until only 27% of bioherm/reef is present at the top. This is the end of the Upper Jurassic. Numerous authors like Gwinner 1976; Geyer and Gwinner 1979; Haq et al. 1987; Meyer and Schmidt-Kaler 1989, 1990; Leinfelder 1993; Leinfelder et al. 1994; Meyer 1994; Ponsot and Vail 1991; have also documented the general trend of increasing–decreasing bioherm/reef growth of the Upper Jurassic in South Germany.

## Discussion

The workflow presented in this study allows using “the sum of magnitude method” to differentiate between potential geothermal reservoir facies (biohermal buildups) and non-reservoir facies (well-bedded basin facies) as there is a very pronounced correlation between the seismic reflectivity and the seismic facies. Biohermal buildups show weak reflectivity and chaotic seismic facies, whereas the non-reservoir facies shows a high



reflectivity and parallel high-amplitude seismic facies. In fact, the non-reservoir facies can always be identified very easily, leaving the conclusion that everything else on the attribute map represents biohermal buildups or debris—the potential geothermal reservoir facies.

The “the sum of magnitude method” is also a method that can be applied relatively quick, especially using the pseudo-stratigraphic layering approach and the attribute analysis per zone. The adjusted maps are the first step to visualize and quantify the distribution of bioherm/reef and basin for each slice allowing the interpreter to understand how the reservoir distribution developed over time. However, “the sum of magnitude method” is not able to differentiate between fault zones and bioherm/reef as both are associated with chaotic seismic facies. Therefore, this approach is only applicable in a non- or only minor faulted setting, focusing on stratigraphic geothermal targets. For example, in karst-dominated systems, these maps provide the first foundation to start thinking about how potential flow zones are distributed, why and where certain targets are present and how they might be connected laterally. Having only limited, potential wellsite locations available on the surface, the first question is if the identified geothermal targets can be reached at all. Therefore, the early integration of these maps into the geothermal exploration process points out very quickly how to optimize the exploration strategy and which potential sweet spots are worth a further, more detailed investigation. As most geothermal companies have only limited financial resources and often only temporary access to software like Petrel, time efficiency is very important. The suggested workflow helps to differentiate very fast between the potential reservoir and non-reservoir facies of Upper Jurassic carbonates in South Germany.

## Conclusion

The workflow of layer-based amplitude extractions and subsequent cut-off definition results in a semi-quantitative method to distinguish basin facies (non-reservoir) from bioherm facies (potential reservoir) on a seismic scale. Comparable results could barely be achieved using manual interpretation on the 3D seismic and would be extremely time-consuming while losing accuracy. The systematic workflow presented in this study is essential to convert the raw output of the seismic attribute maps into meaningful geological maps:

- Reflector termination mapping and standard seismic facies analysis are vital to understand the large-scale depositional architecture and identify critical features (e.g., onlaps of a basin facies with the bioherm/reef).
- Reflectivity correlates with the seismic facies: (a) chaotic seismic facies (bioherm/reef) has a weak reflectivity, and (b) parallel high-amplitude seismic facies (basin) shows a strong reflectivity. The “sum of magnitude” attribute uses the magnitude of the seismic amplitudes (for peak and trough) and hence indicates the reflectivity which can, therefore, differentiate between potential reservoir facies (bioherm/reef) and non-reservoir facies (basin). Fault zones, however, correlate with chaotic seismic facies as well, and can not be distinguished with this method; this is a limitation.
- Creating attribute maps per zone with adjusted cut-offs allows differentiating between the basin and bioherm/reef facies. A thorough comparison of the adjusted

attribute maps with the seismic facies interpretation is required and needs to be applied for multiple crosslines and inlines, and for each zone.

- Comparison with upscaled borehole image logs, well logs, and borehole cuttings confirm the interpretation of the depositional environment and convert the interpretation into a robust geological tool that allows identifying these environments and facies associations on a seismic scale.
- The maps provide now the first foundation to test and discuss geothermal concepts and flow zones, identify potential targets and refine the exploration strategy. They show sediment dispersal trends and how the bioherms prograded–retrograded over time. This is very important as the geothermal projects in Munich get more complex too and multiple geothermal targets in different stratigraphic horizons are needed for sustainable production. At the Schäftlandstraße for example, the Stadtwerke München drilled six highly deviated wells from one wellsite. The attribute maps can be used as input for the next steps of facies modeling, reservoir simulation, and well placement strategy.

Quantitative analysis of 3D seismic data provides a novel tool for the geothermal exploration of carbonate reservoirs. This integrated workflow offers a new approach for systematic geothermal exploration, especially useful in the early exploration stage to quantify and visualize potential geothermal reservoir distribution through time.

#### **Acknowledgements**

We thank Schlumberger for the access to Petrel (trademark of Schlumberger) used for seismic interpretation and modeling. Advanced Logic Technology (ALT) is thanked for providing the WellCAD software used for core description, core to log calibration, borehole image interpretation, and Timo Korth for his exceptional support. Assistance was provided by members of the Sedimentary Geology Group at the University of Tübingen. We are grateful for discussions with many colleagues working on the German Upper Jurassic, notably Dr. M. Nowak and Dr. D. Jung from LfU (Ministry of Environment), and for access to core data. The team from Erdwerk is thanked for their support and for sharing their experience in the Molasse Basin. Stadtwerke München (SWM) is thanked, notably Sebastian Dirner, for access to data and of course all colleagues and friends from the Geothermal Alliance Bavaria (GAB), especially Daniela Pfrang, Dr. Daniel Bohnsack and Dr. Martin Potten. Fabian Setzer (Vulcan Energy Subsurface Solutions) is thanked very much for the additional support and for sharing his seismic interpretation skills and exploration experience, as well as Prof. Dr. Michael Pöppelreiter for his support and advice during the review.

#### **Author contributions**

Philipp Wolpert (Leading), Thomas Aigner (supporting), Daniel Bendias (supporting), Kilian Beichel (supporting) and Kai Zosseder (supporting). All authors read and approved the final manuscript.

#### **Funding**

This work is part of an integrated research project funded by the Geothermal Alliance Bavaria (GAB) and the University of Tübingen. We thank both institutes for funding and permission to publish.

#### **Availability of data and materials**

The Geothermal-Alliance Bavaria (GAB) is thanked for providing the data of this study. The Stadtwerke Munich (SWM) is gratefully thanked for sharing their data and 3D seismic survey.

#### **Declarations**

##### **Competing interests**

There are no competing interests.

Received: 8 March 2021 Accepted: 13 October 2022

Published online: 19 November 2022

## References

- Akbar M, Petricola M, Watfa M, Badri M, Charara M, Boyd A, Cassell B, Nurmi R, Delhomme JP, Grace M, Kenyon B, Roestenburg J. Classical interpretation problems: evaluation carbonates: schlumberger. *Oilfield Rev.* 1995;7:38–57.
- Bachmann GH, Müller M, Weggen K. Evolution of the molasse basin tectonophysics. Amsterdam: Elaviser; 1987. p. 77–92.
- Bendias D, and F. Contreras, 2017, Sedimentology and architecture of deepwater turbidite systems offshore mozambique—from concept to application., PESGE African E&P Conference. London, UK, 31 1st 2017.
- Blakey, R., 2015, Colorado plateau geosystems, Inc. Reconstructing the ancient EARTH, Accessed 04 April 2019 <http://cpgeosystems.com>.
- Böhm F, Savvatis A, Steiner U, Schneider M, Koch R. Lithofazielle Reservoircharakterisierung zur geothermischen Nutzung des Malm im Großraum München Grundwasser. Berlin: Springer; 2013. p. 3–13.
- Böhm F, Birner J, Steiner U, Koch R, Sobott R, Schneider M, Wang A. Thick-bedded dolomitic upper jurassic (Malm) in the moosburg SC4 well: a key for interpreting flow rats in geothermal wells in the malm aquifer (Molasse basin, Germany). *J Geol Sci.* 2011;39(2):117–57.
- Braun AR. Seismic attributes and their classification Lead Edge. Texas: Society of exploration geophysicists; 1996. p. 1090.
- Catuneanu O, Galloway WE, St CGC, Kendall AD, Miall HW, Posamentier AS, Tucker ME. Sequence stratigraphy: methodology and nomenclature newsletters on stratigraphy. Amsterdam: Elsevier; 2011. p. 173–245.
- Chopral S, Marfurt KJ. Seismic attributes—a historical perspective geophysics. Texas: Society of Exploration Geophysicists; 2005. p. 3–28.
- Chen Q, Sidney S. Seismic attribute technology for reservoir forecasting and monitoring. Lead Edge. 1997;16(445):456.
- Chitale VD, Johnson C, Entzminger D, Canter L. Application of a modern electrical borehole imager and a new image interpretation technique to evaluate the porosity and permeability in carbonate reservoirs a case history from the permian basin United States. In: Pöppelreiter M, editor. Dipmeter and borehole image log technology, vol. 92. Tulsa: AAPG Memoir; 2010. p. 1–13.
- Chiracal, T., 2020, Carbonate geo-body dimensions and lateral facies heterogeneities from the SW German upper Jurassic: a satellite and outcrop based analogue study for deep geothermal exploration, student technical congress 2020 organized by the German Section of the Society of Petroleum Engineers, Online Conference, 5–6 November 2020.
- Dunham RJ. Classification of carbonate rocks according to depositional texture. In: Ham WE, editor. Classification of carbonate rocks. Tulsa: AAPG Memoir; 1962. p. 108–21.
- Dussel, M., Moeck, I., Wolfgramm, M., and R. Straubinger. (2018) Characterization of a Deep Fault Zone in Upper Jurassic Carbonates of the Northern Alpine Foreland Basin for Geothermal Production (South Germany). PROCEEDINGS, 43rd Workshop on Geothermal Reservoir Engineering Stanford University, Stanford, California, 1–8.
- Gwinner MP. Origin of the Upper Jurassic of the Swabian Alb: Contrib. Stuttgart: Sedimentology. Schweizerbart'sche Verlagsbuchhandlung; 1976.
- Geyer OF, Gwinner MP. Die Schwäbische Alb und ihr Vorland. Stuttgart: Sammlung Geologischer Führer Schweizerbart'sche verlagsbuchhandlung; 1979. p. 121.
- Gygi RA. Mineralostratigraphy, litho- and biostratigraphy combined in correlation of the Oxfordian (Late Jurassic) formations of the Swiss Jura range. *Eclogae Geol Helv.* 1986;79(2):385–454.
- Hanford CR, Loucks RG. Carbonate depositional sequences and system tracts—response of carbonate platforms to relative sea-level changes: chapter 1. Tulsa: AAPG Memoir; 1993. p. 41.
- Haq BU, Hardenbol J, Vail PR. Chronology of fluctuating sea levels since the triassic Science. Washington: American association for the advancement of science; 1987. p. 1156–67.
- Kerns C, Tinker S. Sequence stratigraphy and characterization of carbonate reservoirs. SEPM Short Course. 1997;40:130.
- Leinfelder RR. Upper Jurassic reef types and controlling factors a preliminary report Profil. Stuttgart: Universit[un]t Stuttgart; 1993. p. 45.
- Leinfelder RR, Werner W, Nose M, Schmid DU, Krautter M, Laternser R, Takacs M, Hartmann D. Paleoecology, growth parameters and dynamics of coral sponge and microbolite reefs from the Late Jurassic Göttinger Arb Geol Paläont. Berlin: Springer; 1996.
- Leinfelder RR, Leinfelder M, Krautter M, Laternser R, Nose M, Schmid D, Schweigert G, Werner W, Keupp H, Brugger H, Herrmann R, Rehfeld-Kiefer U, Schroeder JH, Reinhold C, Koch R, Zeiss A, Schweizer V, Christmann H, Menges G, Lutherbacher H. The origin of Jurassic reefs: current research development and results facies. Berlin: Springer; 1994. p. 56.
- Lemke, 1988 Das bayerische Alpenvorland vor der Eiszeit. Geologie von Bayern I 115 S. Stuttgart. <https://www.abebooks.com/Geologie-Bayern-bayerische-Alpenvorland-Eiszeit-Erdgeschichte-Bau-Bodensch%C3%A4tze/31243327617/bd>
- Mattioni L, Chauveau A, Fonta O, Ryabchenko V, Sokolov E, Mukhametzyanov R, Shlionkin S, Zereninov V, Bobb I. A 3-D fracture model of the kuyumba oil field (eastern Siberia) reflecting the clay and bed thickness-related fracture-density variations of its dolomite reservoir. In: Pöppelreiter M, editor. Dipmeter and borehole image log technology. Tulsa: AAPG Memoir; 2009. p. 17.
- Meyer RKF, Moosburg SC4, die erste Kernbohrung durch den Malm unter der bayerischen Molasse. Erlanger Geologische Abhandlungen. 1994;123:51–81.
- Meyer RKF, Schmidt-Kaler H. Paläogeographie und Schwammriffentwicklung des süddeutschen Malm—ein Überblick: Facies. Berlin: Springer; 1990. p. 175.
- Mitchum RM Jr, Vail PR. Seismic stratigraphic interpretation procedures. In: Payton CE, editor. Seismic stratigraphy—Applications to hydrocarbon exploration. Tulsa: AAPG Memoir; 1977. p. 135.
- Meyer RKF, Schmidt-Kaler H. Paläogeographischer atlas des süddeutschen Oberjura (Malm) Geol Jb. Stuttgart: Schweizerbart'sche verlagsbuchhandlung; 1989. p. 3–77.
- Pawellek T, Aigner T. Stratigraphic architecture and gamma-ray logs of deeper ramp carbonates (Upper Jurassic, SW Germany). *Sed Geol.* 2003a;159:203–40.
- Pawellek T, Aigner T. Apparently homogenous, reef"-limestones built by high-frequency cycles Upper Jurassic, SW-Germany. *Sediment Geol.* 2003b;160:259–84.
- Pawellek T, Aigner T. Dynamic stratigraphy as a tool in economic mineral exploration: ultra-pure limestones (Upper Jurassic, SW Germany) Marine and Petroleum Geology. Amsterdam: Elsevier; 2004. p. 499.

- Pittet B, Strasser A. Depositional sequences in deep-shelf environments formed through carbonate-mud import from the shallow platform (late oxfordian eclogae geologicae helvetiae oxford german Swabian Alb and eastern Swiss Jura). Oxford: Swiss geological society; 1998. p. 69.
- Pittet B, Strasser A, Mattioli E. Depositional sequences in deep shelf environments: a response to sea-level changes and shallow-platform carbonate productivity (Oxfordian, Germany and Spain). *J Sediment Res.* 2000;10(2):392–407.
- Ponsot CM, Vail PR. Sequence stratigraphy of the Jurassic: new data from the Paris-London basin compiled from well logs. *AAPG Bull.* 1991;75:655.
- Pross J, Elmar E, Ruf M, Aigner T. Delineating sequence stratigraphic patterns in deeper ramp carbonates: quantitative palynofacies data from the upper Jurassic (Kimmeridgian) of Southwest Germany. *J Sediment Res.* 2006;76:524–38.
- Quenstedt FA. Der Jura. Tübingen: Tübingen. Laupp und Siebeck; 1858. p. 842.
- Ruf M, Link E, Pross J, Aigner T. Integrated sequence, stable isotope and palynofacies analysis in deeper epicontinental shelf carbonates from the upper Jurassic of SW Germany. *Sediment Geol.* 2005;175:391–414.
- Schlager W. Accommodation and supply-a dual control on stratigraphic sequences. In: Cloetingh S, Sassi W, Horvath F, Puigdefabregas C, editors. *basin analysis and dynamics of sedimentary basin evolution: sedimentary geology*, vol. 86. Amsterdam: Elsevier; 1993. p. 111–36.
- Scotese CR. Atlas of earth history paleogeography. Texas: PALEOMAP Project; 2001. p. 52.
- Steiner, U. and F. Böhm, 2011, Lithofacies and structure signatures of image log in carbonates and their implications for reservoir characterization in Southern Germany: 1st Sustainable Earth Sciences Conference & Exhibition, Valencia, Spain, November 8–11, 2011.
- Strasser A. Ooids in Purbeck limestones (lowermost Cretaceous) of the Swiss and French Jura. *Sedimentology.* 1986;33(5):711–27.
- Strasser A, Davaud E. Black pebbles of the Purbeckian (Swiss and French Jura): lithology, geochemistry and origin: eclogae geologicae. Helvetiae. 1983;76:551–80.
- Vail PR. Seismic stratigraphy interpretation procedure. In: Bally AW, editor. *Atlas of seismic stratigraphy*. Tulsa: AAPG Studies in Geology; 1987. p. 1.
- Vail PR, Todd RG, Sangree JB. Seismic stratigraphy and global changes of sea level: part 5. chronostratigraphic significance of seismic reflections: section 2. Appl Seismic Reflect Config Stratigr Interpret Memoir. 1977;26:99–116.
- Van Wagoner JC, Mitchum RM, Campion KM, Rahmanian VD. Siliciclastic sequence stratigraphy in well logs cores, and outcrops concepts for high-resolution correlation of time and facies methods in exploration series, vol. 7. Tulsa: The American association of petroleum geologists; 1990. <https://www.amazon.com/Siliciclastic-Sequence-Stratigraphy-Cores-Outcrops/dp/0891816577>.
- Van Wagoner JC, Posamentier HW, Mitchum RM, Vail PR, Sarg JF, Loutit TS, Hardenbol J. An overview of and key definitions. In: Wilgus CK, Hastings BS, Kendall CGC, Posamentier HW, Ross CA, Van Wagoner JC, editors. *Sea Level Changes—An Integrated Approach*. Tulsa: SEPM Special Publication; 1988.
- Wolpert PJ, Pöppelreiter MC. Borehole-image-log characterization of deltaic deposits from a behind-outcrop well: opportunities and limitations. *J Sediment Res.* 2019;89:1207–30.
- Wolpert, P.J., Aigner, T., Beichel, K., and D. Bendias, 2019a, Borehole image logs applied to sequence stratigraphy and geothermal exploration in carbonates: an integrated workflow (Upper Jurassic/ Molasse basin). EAGE Third Borehole Geology Workshop. Muscat, Oman, October 14–17 2019a.
- Wolpert, P.J., Aigner, T., Beichel, K., Bendias, D., Steiner, U., and A. Savvatis, 2019b, Linking 3D seismic interpretation and borehole image facies to unravel sequence stratigraphic architecture of Jurassic carbonates EAGE Annual Conference, London, UK, June 3–7, 2019b.
- Ziegler B. The “White” (Upper) Jurassic in Southern Germany. *Stuttgarter Beiträge Zur Naturkunde.* 1977;26:1–79.
- Ziegler PA. Geological atlas of western and central Europe. The Hague: Shell; 1990.

## Publisher's Note

Springer Nature remains neutral with regard to jurisdictional claims in published maps and institutional affiliations.

**Submit your manuscript to a SpringerOpen<sup>®</sup> journal and benefit from:**

- Convenient online submission
- Rigorous peer review
- Open access: articles freely available online
- High visibility within the field
- Retaining the copyright to your article

---

Submit your next manuscript at ► [springeropen.com](https://www.springeropen.com)